A theoretical and computational study of the anion, neutral, and cation Cu(H_2O) complexes

Mark S. Taylor, Felician Muntean,[a] W. Carl Lineberger, and Anne B. McCoy[b]
JILA and Department of Chemistry and Biochemistry, University of Colorado, Boulder, Colorado 80309

(Received 3 May 2004; accepted 21 June 2004)

An *ab initio* investigation of the potential energy surfaces and vibrational energies and wave functions of the anion, neutral, and cation Cu(H_2O) complexes is presented. The equilibrium geometries and harmonic frequencies of the three charge states of Cu(H_2O) are calculated at the MP2 level of theory. CCSD(T) calculations predict a vertical electron detachment energy for the anion complex of 1.65 eV and a vertical ionization potential for the neutral complex of 6.27 eV. Potential energy surfaces are calculated for the three charge states of the copper-water complexes. These potential energy surfaces are used in variational calculations of the vibrational wave functions and energies and from these, the dissociation energies D_0 of the anion, neutral, and cation charge states of Cu(H_2O) are predicted to be 0.39, 0.16, and 1.74 eV, respectively. In addition, the vertical excitation energies, that correspond to the $4\,^2P \leftarrow 4\,^2S$ transition of the copper atom, and ionization potentials of the neutral Cu(H_2O) are calculated over a range of Cu(H_2O) configurations. In hydrogen-bonded, Cu-HOH configurations, the vertical excitation and ionization energies are blueshifted with respect to the corresponding values for atomic copper, and in Cu-OH_2 configurations where the copper atom is located near the oxygen end of water, both quantities are redshifted. © *2004 American Institute of Physics.* [DOI: 10.1063/1.1782191]

I. INTRODUCTION

In the preceding paper, hereafter referred to as Paper I, we presented femtosecond photodetachment-photoionization and time-dependent quantum mechanical wave packet investigations of the short-time dynamics of the neutral Cu(H_2O) complex initiated by electron photodetachment from $Cu^-(H_2O)$.[1] Accurate potential energy surfaces and vibrational wave functions for the anion, neutral, and cation Cu(H_2O) complexes were essential ingredients in both interpreting the experimental results and running the quantum dynamical calculations. In this paper, we present high-level *ab initio* electronic structure calculations and calculations of the vibrational energies and wave functions of the anion, neutral, and cation Cu(H_2O) complexes. The present investigation of the properties of the neutral and ionic Cu(H_2O) complexes is also useful for guiding future spectroscopic investigations of these species,[2–6] for improving models of the aqueous solvation of metal atoms and ions, and for understanding the roles of copper in biological systems.[7–9]

While there have been several *ab initio* electronic structure investigations of $Cu^-(H_2O)$,[10] Cu(H_2O)[11–17] and $Cu^+(H_2O)$,[14,18–22] there is a paucity of experimental work on these complexes, perhaps due to the challenges involved in generating and interrogating them. Fuke and co-workers[23,24] have measured the photoelectron spectra of $Cu^-(H_2O)_n$ $(n=1-4)$. They find that the photoelectron spectrum of $Cu^-(H_2O)$ resembles that of Cu^-, shifted to ≈ 0.3 eV higher electron binding energy. The fact that the photoelectron spectrum $Cu^-(H_2O)$ resembles that of Cu^- suggests that this complex is well described as a perturbed copper atomic anion. The photoelectron spectrum yields a vertical detachment energy to the Cu(H_2O) electronic ground-state of 1.58 eV, which enabled Fuke and co-workers to estimate the Cu^--H_2O binding energy to be 0.55 eV. Further experimental evidence of the Cu(H_2O) complex is provided by Margrave and co-workers[25] who co-condensed Cu atoms and H_2O in a cryogenic Ar matrix. They interpreted an IR absorption band, which is shifted 20.5 cm^{-1} to the red of the H_2O bend fundamental of matrix isolated H_2O, as arising from the Cu(H_2O) complex. Finally, the binding enthalpy of $Cu^+(H_2O)$ has been measured by two independent collision-induced dissociation mass spectrometry studies to be 1.5 ± 0.1 eV (Ref. 26) and 1.67 ± 0.08 eV.[27]

In order to interpret more fully the photodetachment-photoionization studies[1] of $Cu^-(H_2O)$ we have carried out a series of computations. First, we calculate the $Cu^-(H_2O)$ anion potential energy surface around the equilibrium geometry. Converged variational calculations are performed to determine the vibrational wave functions and energies of $Cu^-(H_2O)$ and $Cu^-(D_2O)$. We find that the $Cu^-(H_2O)$ ground-state wave function is delocalized between two equivalent Cu-HOH hydrogen bonded configurations. The CCSD(T) calculated dissociation energy of $Cu^-(H_2O)$ is 0.39 eV and vertical detachment energy to the electronic ground-state of Cu(H_2O) is 1.65 eV.

Photodetachment of an electron from $Cu^-(H_2O)$ produces neutral Cu(H_2O) with an internal energy that is comparable to the Cu-H_2O dissociation energy and, as a result, the wave packets that are generated upon photodetachment of an electron from $Cu^-(H_2O)$ can sample all of the attrac-

[a]Permanent address: Varian Corporation, Walnut Creek, CA.
[b]Permanent address: Department of Chemistry, The Ohio State University, Columbus, OH.

tive regions of the neutral surface. This necessitates calculation of the global Cu(H_2O) potential energy surface for use in the quantum wave packet calculations that are described in Paper I.[1] We calculate a dissociation energy for the Cu(H_2O) complex of 0.16 eV, using the CCSD(T) method. Based on a calculation of the photoelectron spectrum, we find that when the anion has an initial vibrational temperature of 200 K, 50% of the population on the neutral surface is in vibronic states that have total internal energies in excess of the Cu $+H_2O$ dissociation energy.

In order to connect the time-dependent photoionization signals obtained in our experiment with the dynamics of neutral Cu(H_2O), we explore the nature of the intermediate states involved in the resonant multiphoton ionization of neutral Cu(H_2O) over the range of configurations that the complex explores following photodetachment of the anion. The results of *ab initio* calculations[28] and experimental studies[29–33] agree that both the resonant transition and the vertical ionization energies shift markedly with the H_2O orientation and the Cu-H_2O distance. We use time-dependent density functional theory to estimate the relevant Cu(H_2O) transition energy. We find that the Cu "pseudo $4P \leftarrow 4S$" resonance transition is blueshifted by up to 0.14 eV from the atomic value in Cu-H_2O configurations, and it is redshifted by as much as 1.91 eV in Cu-OH_2 configurations at short Cu-OH_2 separations. We also calculate a vertical ionization energy surface for neutral Cu(H_2O) and find that its ionization potential is blueshifted from the atomic value by as much as 0.36 eV in Cu-H_2O configurations, and redshifted from the atomic value by up to 1.87 eV in Cu-OH_2 configurations. Finally, $Cu^+(H_2O)$ is found to have a planar C_{2v} Cu-OH_2 geometry and a CCSD(T) dissociation energy of 1.74 eV.

II. THEORETICAL AND COMPUTATIONAL DETAILS

We divide the discussion of the theoretical and computational details into three parts: a discussion of the electronic structure methods used to study the copper-water complex, the vibrational Hamiltonian for this system, and how we couple these two parts through the generation of potential surfaces for the anionic, neutral, and cationic Cu(H_2O) complexes.

A. Electronic structure calculations

Electronic structure calculations are performed using the GAUSSIAN 98 program package.[34] The 10 core electrons and 19 valence electrons of copper are represented by a relativistic effective core potential (RECP) and $(7s,7p,6d,3f)$ valence basis set, referred to as aug-SDB.[35] This valence basis set comprises 79 basis functions. The Stuttgart-Dresden-Bonn (SDB) RECP and corresponding $(6s,5p,3d)$ basis set for Cu were developed by Preuss and co-workers.[36] In their study of anion and neutral CuX_2 $(X=\mathrm{Cl,Br})$, Wang and coworkers partially decontracted and augmented the SDB valence basis set to yield the $(7s,7p,6d,3f)$ basis set that is used in the present study.[35] Hydrogen and oxygen are represented by the augmented correlation-consistent polarized valence triple ζ basis set, aug-cc-pVTZ.[37]

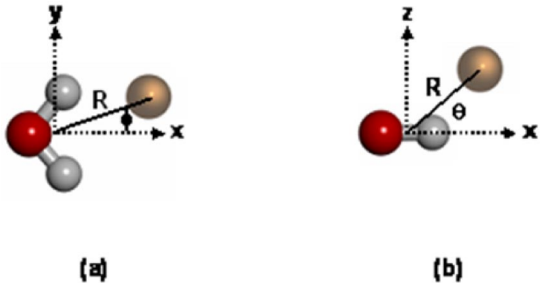

FIG. 1. The coordinates used in this study. In the Cu-H_2O C_{2v} configuration, $\theta=90°$ while $\phi=0°$.

All structures are optimized with second-order Møller-Plesset perturbation theory (MP2), with only valence electrons correlated, using analytical gradients. Geometries of minima and transition states are converged using the "very tight" gradient convergence criteria of GAUSSIAN 98. Slices through the anion, neutral, and cation Cu(H_2O) potential energy surfaces are generated at the MP2 level of theory by varying the Cu-H_2O separation and minimizing the energy with respect to the intramolecular coordinates of the water molecule at each point. In these calculations, the standard GAUSSIAN 98 gradient convergence criteria are used for computational economy.

The dissociation energies from the minimum (D_e) and zero-point level (D_0) of the anion, neutral, and cation Cu(H_2O) complexes and the vertical detachment energy (VDE) of $Cu^-(H_2O)$ and vertical ionization energy (VIE) of Cu(H_2O) are evaluated using both MP2 and the coupled cluster theory with single and double excitations and perturbative triple excitations, CCSD(T), correlating only the valence electrons. Here we use VDE and VIE to refer to calculations of the detachment and ionization energies at fixed Cu(H_2O) geometries. When evaluating D_0, we use the zero-point energies that are obtained from our converged variational calculations for the intermolecular vibrations, described below, and exclude the zero-point vibrational energy contributions from the H_2O intramolecular modes. This approach has the advantage of avoiding the errors associated with harmonic vibrational frequencies. In addition, the vertical electronic excitation energies of Cu(H_2O) are calculated using an implementation of the time-dependent density-functional theory, using the Becke3–Lee–Yang–Parr (B3LYP) hybrid functional.[38–40]

B. Vibrational coordinates and hamiltonian

Since the intramolecular vibrational motions of water are fast compared to the intermolecular vibrations, we consider only the intermolecular vibrations in our treatment of the Cu(H_2O) complexes. As such, the vibrational Hamiltonian depends only on three coordinates. These are the distance between the copper atom and the center of mass of the water molecule, R; the orientation of the copper atom relative to a vector that is perpendicular to the water molecule, θ; and the vector that connects the oxygen atom to the center of mass of water, ϕ. These coordinates are illustrated in Fig. 1.

In this representation of the copper-water complex, the Hamiltonian is given by

$$\hat{H} = -\frac{\hbar^2}{2\mu_R}\frac{\partial^2}{\partial R^2} + \frac{2\pi c}{\hbar}[b_x\hat{j}_x^2 + b_y\hat{j}_y^2 + b_z\hat{j}_z^2] + \frac{|\hat{J}-\hat{j}|^2}{2\mu_R R^2} + V(R,\theta,\phi)$$
$$= -\frac{\hbar^2}{2\mu_R}\frac{\partial^2}{\partial R^2} + \frac{2\pi c}{\hbar}\left[\frac{b_x+b_y}{2}(\hat{j}^2-\hat{j}_z^2) + \frac{b_x-b_y}{4}(\hat{j}_+^2+\hat{j}_-^2) + b_z\hat{j}_z^2\right] + \frac{|\hat{J}-\hat{j}|^2}{2\mu_R R^2} + V(R,\theta,\phi). \quad (1)$$

Here, μ_R represents the reduced mass of the copper-water complex, while the b_α give the vibrationally averaged rotational constants of water. In the present coordinate system, $b_x = 27.88$; $b_y = 14.51$; and $b_z = 9.28\ \mathrm{cm}^{-1}$ for H_2O (Ref. 41) and $b_x = 15.25$; $b_y = 7.30$; and $b_z = 4.94\ \mathrm{cm}^{-1}$ for D_2O. Finally, $V(R,\theta,\phi)$ represents the intermolecular potential for this system, obtained from the electronic structure calculations. Because the coordinate system is referenced to the center of mass of water, slightly different potentials are used for the complexes with H_2O and D_2O.

The development of the potentials is described in detail below. For the anion and neutral complexes and for the vertical ionization surface, the potential energy surface takes the form

$$V(R,\theta,\phi) = \sum_{l,m} v_{l,m}(R)\frac{1}{\sqrt{2(1+\delta_{m,0})}} \times [y_{l,m}(\theta,\phi) + (-1)^m y_{l,-m}(\theta,\phi)], \quad (2)$$

where $y_{l,m}(\theta,\phi)$ are the spherical harmonics.[42] Since, in the case of the cation we are only interested in the ground state and fundamentals, we do not fit the surface, but use a spline interpolation of the *ab initio* points.

Based on the forms of the kinetic energy operator and the potential, a convenient representation for the Hamiltonian matrix is to use a discrete variable representation (DVR) in R (Refs. 43 and 44) while the angular dependences are expanded in terms of symmetrized Wigner rotation matrices.[42] As we only consider cases where $J=0$, these reduce to linear combinations of spherical harmonics:[42]

$$\langle\theta,\phi|j,k,\varepsilon\rangle = \frac{1}{\sqrt{2(1+\delta_{k,0})}} \times [y_{j,k}(\theta,\phi) + \varepsilon(-1)^k y_{j,-k}(\theta,\phi)], \quad (3)$$

where $\varepsilon = \pm 1$, and defines the parity of the system.

C. Computational details

1. Anion

The construction of the potential for $Cu^-(H_2O)$ takes place in two stages. First we calculate a slice through this surface in R, with $\theta = 90°$ and $\phi = 0°$. Here the potential is calculated at the MP2 level using the basis described above, with R in a range from 2.2 to 7.5 Å, in increments of 0.1 Å. For calculations involving this surface, we employ a cubic spline to interpolate between the calculated points.[45]

In addition, the potential is calculated as a function of θ and ϕ with $30° \leqslant \theta \leqslant 90°$ and $0° \leqslant \phi \leqslant 100°$, in increments of 10°. In this case, R and the intramolecular coordinates of the water molecule are allowed to vary in order to minimize the interaction energy. For each of the seven values of θ for which the potential is calculated, the values of $V(\theta,\phi)$ are fit to an expansion in $\cos(m\phi)$ with $m \leqslant 3$. This expression is inverted to give an expansion in normalized associated Legendre polynomials, $\Theta_{l,m}(\theta)$,

$$V(\theta,\phi) = \sum_{m=0}^{3} V_m(\theta)\cos(m\phi),$$
$$V_m(\theta) = \sum_{l=0}^{6} v_{l,m}\sqrt{\frac{\pi}{2}}[\Theta_{l,m}(\theta) + (-1)^m\Theta_{l,-m}(\theta)]. \quad (4)$$

This separation of the radial and angular dependencies of the potential is justified by the fact that at vibrational temperatures below 200 K the anion nuclear wave functions are localized near the potential minimum. Over the range of angles that are sampled by $Cu^-(H_2O)$ at 200 K, the minimum value of R changes by less than 0.1 Å.

The vibrational wave functions and energies for $Cu^-(H_2O)$ are obtained in two steps. As noted above, the potential is expressed as the sum of a radial and angular contribution and Eq. (2) becomes

$$V(R,\theta,\phi) = V_{rad}(R) + \sum_{l,m} v_{l,m}\frac{1}{\sqrt{2(1+\delta_{m,0})}} \times [y_{l,m}(\theta,\phi) + (-1)^m y_{l,-m}(\theta,\phi)]. \quad (5)$$

As such, with the exception of the second to the last term in Eq. (1), which is proportional to $\hat{j}^2/R^2$, the stretch and bend contributions to the Hamiltonian are separable. Taking advantage of this separability, we define

$$h_j^{(R)} = -\frac{\hbar^2}{2\mu_R}\frac{\partial^2}{\partial R^2} + \frac{\hat{j}^2}{2\mu_R R^2} + V_{rad}(R) \quad (6)$$

for each value of j. We solve for the energy and wave functions using a DVR of 200 evenly spaced grid points between 2.40 and 7.17 Å.[44] We save the lowest 20 wave functions, $\psi_{n,j}(R)$, and use these functions to evaluate the full Hamiltonian

$$\hat{H} = \hat{h}_j^{(R)} + \frac{2\pi c}{\hbar}\left(\frac{b_x+b_y}{2}\right)[\hat{j}^2-\hat{j}_z^2] + \frac{2\pi c}{\hbar}\left(\frac{b_x-b_y}{4}\right) \times [\hat{j}_+^2+\hat{j}_-^2] + \frac{2\pi c}{\hbar}b_z\hat{j}_z^2 + \sum_{l,m} v_{l,m}\frac{1}{\sqrt{2(1+\delta_{m,0})}} \times [y_{l,m}(\theta,\phi) + (-1)^m y_{l,-m}(\theta,\phi)] \quad (7)$$

in a direct product basis

$$|n,j,k,\varepsilon\rangle = |\psi_{n,j}\rangle|j,k,\varepsilon\rangle. \quad (8)$$

We find that for $Cu^-(H_2O)$, including all angular functions with $j \leqslant 15$ is sufficient, while for $Cu^-(D_2O)$, we include functions with $j \leqslant 25$. Finally, since the center of mass of

water changes upon deuteration, we shift the radial dependence of the potential by 0.0424 Å to reflect this change in the definition of R for D_2O.

2. Neutral

Unlike the potential for the anion, the nature of the neutral surface does not permit a simple separation of the angular and radial dependencies of the potential. As a result, in this case, slices through the potential along R are calculated for $\theta=0°$, 30°, 60°, and 90° and $\phi=0°$, 45°, 90°, 135°, and 180° in increments of 0.2 Å, starting on the repulsive wall of the Cu(H_2O) potential. Additional points, spaced by either 0.05 or 0.1 Å, are also calculated near the minimum of each slice. The resulting 16 curves (when $\theta=0°$ the potential does not depend on ϕ) are each fit to the following equation:

$$\begin{aligned} V(R)&=V_M(R)S(R)+V_D(R)[1-S(R)],\\ V_M(R)&=D_e[e^{-2\beta(R-R_M)}-2e^{-\beta(R-R_M)}]+E_M,\\ V_D(R)&=\sum_{i=2}^{5}\frac{c_{2i}}{R^{2i}},\\ S(R)&=\frac{e^{-\alpha(R-R_S)}}{e^{\alpha(R-R_S)}+e^{-\alpha(R-R_S)}}. \end{aligned} \tag{9}$$

We then use the potential to calculate the low-lying vibrational energies and wave functions for Cu(H_2O). Because the stretch/bend coupling is stronger in the neutral than in the anion, we use a sequential diagonalization and truncation approach in which we start[46,47] by obtaining the bend energies and wave functions for a set of fixed values of R by solving

$$\hat{h}_{ang}=\frac{2\pi c}{\hbar}[b_x\hat{j}_x^2+b_y\hat{j}_y^2+b_z\hat{j}_z^2]+\frac{\hat{j}^2}{2\mu_R R^2}+V(R,\theta,\phi) \tag{10}$$

in a basis of spherical harmonics that includes all states with $j\leqslant 20$ for H_2O and $j\leqslant 30$ for D_2O. These are calculated for 200 values of R ranging from 1.0 to 12.2 Å. The lowest 20 states are retained and provide the bend basis functions for each of the DVR points in the evaluation of the full Hamiltonian matrix. Using this approach, the energies are converged to better than 0.05 cm^{-1}.

3. Cation

Two surfaces are generated for the cation. The first is the vertical ionization energy surface. In this case, we calculate the energy difference between the $Cu^+(H_2O)$ and Cu(H_2O) surfaces as a function of the three intramolecular coordinates, with the water geometry fixed at its minimum energy structure in the neutral complex. As such, this surface represents the energy that is required to remove an electron from the complex without allowing the water to relax. We fit the vertical ionization energy surface using the same approach as we used to generate the neutral surface. In contrast to the neutral surface, we employ a spline interpolation[45] to evaluate the cuts at other Cu-H_2O distances. The angular dependence of this surface is obtained by inverting the 16 cuts at fixed orientations to an expansion in terms of 16 spherical harmonics, as described above.

Finally, we calculate the potential for $Cu^+(H_2O)$ near the Cu-OH_2 global minimum energy structure. In this case, the water geometry is allowed to relax in order to minimize the total energy. Near the minimum energy structure, the radial and angular motions are essentially decoupled. Therefore, we follow the same procedure as is described above for calculating the energies of the anion and consider the radial and angular components separately. The radial dependence is obtained through a one-dimensional cut through the potential at the C_{2v} Cu-OH_2 geometry. The angular dependence of the potential is calculated for $30°<\theta<90°$ in increments of 5° and for $\theta=0°$ and 20°. Except for when $\theta=0°$, where the potential is independent of ϕ, the potential is evaluated for $120°<\phi<180°$, again in increments of 5°. To calculate energies for the cation, the potential is interpolated over this range using a two-dimensional spline. Since $\phi=120°$ is in the repulsive region of the potential, the low-lying states do not sample smaller values of this angle. Since the low-lying wave functions are not expected to sample values of ϕ that are smaller than 120°, for these geometries we set the potential equal to its value at $\phi=120°$. The necessary integrals of the potential over the basis functions in Eq. (3) are evaluated using a 96 point Gauss-Legendre quadrature in θ and 200 points evenly spaced between 0° and 180° degrees in ϕ. We find that the energies are converged to better than 0.1 cm^{-1}, when a basis with $j\leqslant 20$ is used for $Cu^+(H_2O)$ and $j\leqslant 30$ is used for $Cu^+(D_2O)$.

The *ab initio* points and the parameters for the potential surfaces for the three charge states of Cu(H_2O), the vertical ionization surface of neutral Cu(H_2O), and the energies of the 20 lowest vibronic states of the anion and neutral for both Cu(H_2O) and Cu(D_2O) are available from EPAPS.[48]

III. RESULTS AND DISCUSSION

A. Calibration of electronic structure calculations

In order to interpret fully the photodetachment-photoionization experiments on Cu(H_2O), we require accurate $Cu^-(H_2O)$ vibrational wave functions, a high quality global neutral Cu(H_2O) potential energy surface and vertical ionization energy surface that describes how the ionization energy of Cu(H_2O) varies across the neutral potential energy surface. We distinguish between those properties that are calculated as differences between the energies of species in different electronic states or with different numbers of electrons, such as electron affinity, excitation energy, and ionization energy, and those properties that are calculated as differences between the energies of species in the same electronic state, such as potential energy surfaces and vibrational wave functions. We expect that accurate calculation of the former properties will require a high-level treatment of electron correlation such as CCSD(T), whereas accurate calculation of the latter properties may be carried out with an electron correlation treatment such as MP2. To choose an appropriate level of theory for these *ab initio* calculations, the aug-SDB basis set and RECP[35] is tested in conjunction with the MP2, CCSD(T), and TDB3LYP methods for calculating the properties of atomic copper. The results are summarized in Table I.

TABLE I. Calculated properties of atomic copper.

	Electron affinity (eV)	Ionization potential (eV)	^2S-^2P transition energy (j-averaged) (eV)	^2S-^2D transition energy (j-averaged) (eV)
MP2	0.90	7.78	···	···
CCSD(T)	1.20	7.74	···	···
TDB3LYP	···	···	4.13	1.17
Expt.[a]	1.24	7.73	3.81	1.49

[a]The experimental electron affinity is from Haugen (Ref. 69). The experimental ionization potential is from Lide *et al.* (Ref. 70). The ^2S-^2P and ^2S-^2D transition energies are from the NIST Atomic Spectral Database (Ref. 49) and j averaged.

The excellent agreement between the CCSD(T)/aug-SDB and experimental atomic electron affinity and ionization potential provides confidence that this level of theory will predict accurate properties such as the vertical detachment and ionization energies of the $Cu(H_2O)$ anion and neutral, respectively. It also provides confidence that the aug-SDB basis provides an accurate description of the copper electronic structure. While the coupled cluster calculations are of high accuracy, they are too computationally expensive to use in the large number of calculations required to construct potential energy surfaces, and so we use MP2 calculations of the anion and neutral potential energy surfaces and for the vertical ionization surface of $Cu(H_2O)$. MP2/aug-SDB overestimates the ionization potential of the copper atom by 0.06 eV, an error of less than 1%, leading us to expect that we can obtain an accurate description of the vertical ionization surface at this level of theory.

A calculation of the vertical excitation energy of the neutral $Cu(H_2O)$ complex at varying geometries is essential for a compelling interpretation of the time-dependent photoionization signals. For this purpose, time-dependent density functional theory (TDB3LYP) is tested in its prediction of the atomic copper $4\,^2P \leftarrow 4\,^2S$ excitation energy. We find that it overestimates the j-averaged atomic transition energy[49] of 3.81 eV by 0.32 eV, but subtraction of this constant from calculated excitation energies of $Cu(H_2O)$ will allow a qualitative discussion of the vertical excitation energies of the $Cu(H_2O)$ complex.

B. Anion, neutral, and cation $Cu(H_2O)$ stationary points and energetics

When calculating the dissociation energies and potential energy surfaces of the three charge states of the $Cu(H_2O)$ complexes, there are four energetic corrections that must be considered. First, the vibrational zero-point energy of the complexes must be taken into account. As discussed, in evaluating D_0 we exclude the H_2O zero-point energy, use the intermolecular Cu-H_2O MP2 potential energy surfaces to calculate the intermolecular zero-point vibrational energy for each charge state, and use this to evaluate dissociation energies (D_0) at both the MP2 and CCSD(T) levels of theory. The second correction arises from incomplete treatment of electron correlation. We account for electron correlation by the MP2 and CCSD(T) levels of theory, and report both energies in our subsequent discussion in the format MP2/CCSD(T). The third and fourth corrections, basis set superposition error (BSSE) and basis set incompleteness error (BSIE), arise from the use of incomplete basis sets to describe both Cu and H_2O. We evaluate the effects of BSSE on the D_0 and the potential energy surfaces of the three charge states of $Cu(H_2O)$[50] using the counterpoise technique of Boys and Bernardi,[51] with relaxed fragment geometries.[52] In accordance with previous studies on Cu-ligand complexes,[11,15,53–55] we find that correction for BSSE decreases the binding energy of the anion, neutral, and cation complexes, by as much as 40% for neutral $Cu(H_2O)$. Table II shows that going from MP2 to CCSD(T) increases the binding energy of neutral $Cu(H_2O)$ while decreasing the binding energies of anion and cation $Cu(H_2O)$. As the BSSE correction opposes the electron correlation correction for neutral $Cu(H_2O)$, and there is no way of assessing the BSIE of the complexes, we choose to heed the advice of expert practitioners[56] who state that the BSSE uncorrected D_0 is often closer to the actual value than the BSSE corrected D_0. In all of our quoted D_0's and all of our anion, neutral, and cation $Cu(H_2O)$ potential energy surfaces we use the MP2 or CCSD(T) energies without the BSSE correction.

TABLE II. Dissociation energies of $Cu(H_2O)$ anion, neutral and cation stationary points.

	MP2[a] (cm^{-1}, eV)	CCSD(T)[a] (cm^{-1}, eV)	MP2 Zero-point energy[b] (cm^{-1}, eV)
$Cu^-(H_2O)$	4300	3750	625
Minimum (C_s)	0.53	0.46	0.078
$Cu^-(H_2O)$	4100	3600	···
Transition state (C_{2v})	0.51	0.45	···
$Cu(H_2O)$	1600	1750	463
Global minimum (C_s)	0.20	0.22	0.057
$Cu(H_2O)$	1300	1450	···
Transition state (C_{2v})	0.16	0.18	···
$Cu(H_2O)$	400	350	···
H-bonded minimum (C_s)	0.05	0.05	···
$Cu^+(H_2O)$	15350	14600	607
Minimum (C_{2v})	1.90	1.81	0.075

[a]All energies are reported to the nearest 50 cm^{-1} (top entry) and 0.01 eV (bottom entry).

[b]Zero-point energies are calculated by solving Eq. (1) for the energy of the ground vibrational state and are reported to the nearest 1 cm^{-1} (top entry) and 0.001 eV (bottom entry).

Energies, geometries, and harmonic frequencies of the anion, neutral, and cation $Cu(H_2O)$ stationary points are presented in Tables II and III, respectively. Using MP2 with an all-electron $(10s,8p,4d,1f)$ Cu basis set and 6-31G(d,p) for H_2O, Zhan and Iwata[10] found a C_{2v} minimum for $Cu^-(H_2O)$. In contrast, our MP2/(aug-SDB aug-cc-pVTZ) calculations find that H_2O asymmetrically hydrates Cu^-, resulting in a C_s $Cu^-(H_2O)$ minimum, and a C_{2v} first-order saddlepoint. In order to ascertain the minimum energy structure of $Cu^-(H_2O)$, we investigate the effect of varying Cu and H_2O basis sets at the MP2 level of theory. First we use aug-cc-pVTZ for H_2O with three all-electron Cu basis sets[10,57,58] and a 10 electron RECP and $(6s,5p,3d,2f,1g)$ valence Cu basis set[59] and consistently find a C_s minimum

TABLE III. Geometrical parameters and harmonic vibration frequencies for the stationary points of the copper water complexes.[a]

Stationary point	Parameter		Vibration	Cu(H_2O) Harmonic frequencies	Cu(D_2O) Harmonic frequencies	Cu(H_2O) Fundamental frequencies	Cu(D_2O) Fundamental frequencies
$Cu^-(H_2O)$	Cu-H1	2.328	$\omega_1(a')$ bound H stretch	3398	2466	–	–
Global minimum	Cu-H2	3.276	$\omega_2(a')$ HOH bend	1629	1192	–	–
(C_s)	Cu-O	3.257	$\omega_3(a'')$ Cu-H_2O stretch	119	112	105	101
	O-H1	0.986	$\omega_4(a'')$ out-of-plane bend, θ	601	437	728	539
	O-H2	0.964	$\omega_5(a'')$ free H stretch	3843	2796	–	–
	∠HOH	99.0°	$\omega_6(a'')$ in-plane bend, ϕ	245	179	203[b]	137[b]
	R	3.198					
	θ	90.0°					
	ϕ	33.0°					
$Cu^-(H_2O)$	Cu-H	2.696	$\omega_1(a1)$ symmetric H stretch	3687	2662	–	–
Transition state	Cu-O	3.243	$\omega_2(a1)$ HOH bend	1625	1190	–	–
(C_{2v})	O-H	0.972	$\omega_3(a1)$ Cu-H_2O stretch	107	102	–	–
	∠HOH	96.5°	$\omega_4(b1)$ out-of-plane bend, θ	559	410	–	–
	R	3.171	$\omega_5(b2)$ antisymmetric H stretch	3730	2725	–	–
	θ	90.0°	$\omega_6(b2)$ in-plane bend, ϕ	200i	143i	–	–
	ϕ	0.0°					
Cu(H_2O)	Cu-O	2.068	$\omega_1(a'')$ symmetric H stretch	3745	2699	–	–
Global minimum	O-H	0.966	$\omega_2(a')$ HOH bend	1615	1182	–	–
(C_s)	∠HOH	105.3°	$\omega_3(a')$ Cu-H_2O stretch	224	212	187	187
	R	2.108	$\omega_4(a')$ bend in θ	354	272	131[b]	98[b]
	θ	38.6°	$\omega_5(a'')$ antisymmetric H stretch	3872	2838	–	–
	ϕ	180.0°	$\omega_6(a'')$ bend in ϕ	433	315	414	323
Cu(H_2O)	Cu-O	2.067	$\omega_1(a1)$ symmetric H stretch	3766	2713	–	–
Transition state	O-H	0.964	$\omega_2(a1)$ HOH bend	1608	1183	–	–
(C_{2v})	∠HOH	107.1°	$\omega_3(a1)$ Cu-H_2O stretch	211	202	–	–
	R	2.131	$\omega_4(b1)$ out-of-plane bend, θ	274i	210i	–	–
	θ	90.0°	$\omega_5(b2)$ antisymmetric H stretch	3904	2864	–	–
	ϕ	180.0°	$\omega_6(b2)$ in-plane bend, ϕ	344	256	–	–
Cu(H_2O)	Cu-H1	2.555	$\omega_1(a')$ symmetric H stretch	3758	2712	–	–
H-bonded	Cu-H2	3.877	$\omega_2(a')$ HOH bend	1621	1186	–	–
minimum	Cu-O	3.520	$\omega_3(a')$ Cu-H_2O stretch	65	62	–	–
(C_s)	O-H1	0.965	$\omega_4(a'')$ out-of-plane bend, θ	196	141	–	–
	O-H2	0.962	$\omega_5(a'')$ antisymmetric H stretch	3910	2861	–	–
	∠HOH	103.9°	$\omega_6(a'')$ in-plane bend, ϕ	129	93	–	–
	R	3.480					
	θ	90.0°					
	ϕ	53.5°					
$Cu^+(H_2O)$	Cu-O	1.878	$\omega_1(a1)$ symmetric H stretch	3769	2717	–	–
Global minimum	O-H	0.966	$\omega_2(a1)$ HOH bend	1659	1222	–	–
(C_{2v})	∠HOH	107.8°	$\omega_3(a1)$ Cu-H_2O stretch	446	446	437	420
	R	1.942	$\omega_4(b1)$ out-of-plane bend, θ	30	23	197	125
	θ	90.0°	$\omega_5(b2)$ antisymmetric H stretch	3866	2837	–	–
	ϕ	180.0°	$\omega_6(b2)$ in-plane bend, ϕ	622	464	654	479

[a]Bond lengths are in Å, angles in degrees, vibrational frequencies in cm^{-1}.
[b]The frequency was calculated by taking to be the difference between the energy of the state with two quanta in this mode and the average of the energy of ground state and the fundamental.

and C_{2v} first-order saddlepoint. Second, we use the (10*s*,8*p*,4*d*,1*f*) Cu basis set of Iwata[10] and vary the H_2O basis set. We find that small H_2O basis sets such as 3-21G and 6-31G(*d*,*p*) find only a C_{2v} minimum while larger basis sets such as 6-311++G(*d*,*p*), aug-cc-pVTZ, and aug-cc-pVQZ find a C_s minimum and C_{2v} first-order saddlepoint. This suggests that H_2O asymmetrically complexes with Cu^-, with one H-Cu^- hydrogen bond, as in the hydrated halide ions $X^-(H_2O)$.[6] The $Cu^-(H_2O)$ interaction can be understood as having a charge-dipole and hydrogen bonding component. The former interaction favors a C_{2v} minimum and is reproduced using small H_2O basis sets while the latter interaction favors an asymmetric, C_s minimum, and requires large H_2O basis sets to be well described.

Forming a complex with Cu^- perturbs the H_2O molecule by compressing the HOH angle from 104.5° to 99.0° and increases the bound H-O distance by 0.025 Å, to 0.986 Å. It is likely that photodetachment of an electron from $Cu^-(H_2O)$ will result in excitation of the OH stretches and HOH bend in a significant fraction of the neutral Cu(H_2O) complexes. Harmonic frequency analysis shows that the bound H-O stretching frequency is reduced to 3398 cm^{-1}.

The two equivalent C_s minima are connected by a C_{2v} transition state with a barrier of 0.02/0.02 eV. The anion is bound by 0.45/0.39 eV when the zero point energy is taken into account. As discussed above, we shift the CCSD(T) dissociation energy by the zero-point energy, calculated from the MP2 surface. Using the measured $Cu^-(H_2O)$ vertical detachment energy,[23,24] we estimate $D_0[Cu^-(H_2O)]=0.39$ eV which is in excellent agreement with our calculated CCSD(T) value.[60] The CCSD(T) calculated vertical detachment energy of $Cu^-(H_2O)$ is 1.65 eV, which agrees well with the measured value[23,24] of 1.58 eV.

The global minimum on the neutral $Cu(H_2O)$ surface is nonplanar with C_s symmetry. This is in agreement with a previous density functional theory investigation by Papai.[11] The geometry of the H_2O molecule is not significantly perturbed within the complex, although the harmonic vibrational frequencies of H_2O are all redshifted with respect to free H_2O. The antisymmetric stretch, symmetric stretch, and bend are redshifted by 76, 77, and 13 cm^{-1}, respectively. This is consistent with the observed redshift of the HOH bend observed in the matrix-isolation study of $Cu(H_2O)$ by Margrave and co-workers.[25] The two C_s minima are connected by a C_{2v} transition state with a barrier of 0.03/0.03 eV. Previous *ab initio* investigations[11,14,15] of $Cu(H_2O)$ have shown that inclusion of electron correlation increases the binding energy of the complex. We calculate the dissociation energy D_0 of neutral $Cu(H_2O)$ to be 0.14 eV at the MP2 level. If we subtract the MP2 zero point energy from the CCSD(T) D_e, we obtain a D_0 of 0.16 eV and compare this to the most recent values of 0.15 eV (MP4)[15] and 0.16 eV (DFT), both of which include a correction for BSSE.[11] We identify a second minimum, bound by 0.05/0.05 eV, in which the Cu interacts with water via a nonlinear hydrogen bond. In the experiments described in Paper I,[1] $Cu(H_2O)$ is formed by photodetachment of an electron from $Cu^-(H_2O)$. When we calculate the binding energy of $Cu(H_2O)$ at the minimum energy geometry of the anion we find that the vertically detached $Cu(H_2O)$ has an energy 0.01 eV below the energy of dissociated $Cu+H_2O$. This suggests that photodetachment of an electron from $Cu^-(H_2O)$ results in a significant fraction of the neutral $Cu(H_2O)$ complexes having enough internal energy to dissociate.

The minimum of $Cu^+(H_2O)$ has a planar C_{2v} geometry and a calculated dissociation energy D_0 of 1.83/1.74 eV at MP2 and CCSD(T) levels, respectively. These values slightly exceed the experimental ΔH^{298} of 1.67 ± 0.08 eV obtained by Armentrout and co-workers,[27] also the CCSD(T) ΔH^{298} of 1.67 eV calculated by Feller and co-workers.[20] The difference possibly reflects the neglect of BSSE in the present calculations.

At the CCSD(T) level of theory, we calculate a 6.27 eV vertical ionization energy (VIE) for equilibrium neutral $Cu(H_2O)$. This represents a 1.47 eV redshift relative to the ionization potential of Cu, calculated at the same level of theory. In contrast, the vertically detached cation (at the C_{2v} anion geometry) has an energy that is 0.38 eV above the energy of the separated Cu^+ and H_2O fragments. This is due to the repulsive interaction between Cu^+ and the water hydrogens, and suggests that $Cu^+(H_2O)$ formed by ionization of complexes with Cu-HOH configurations is likely to dissociate into Cu^+ and H_2O.

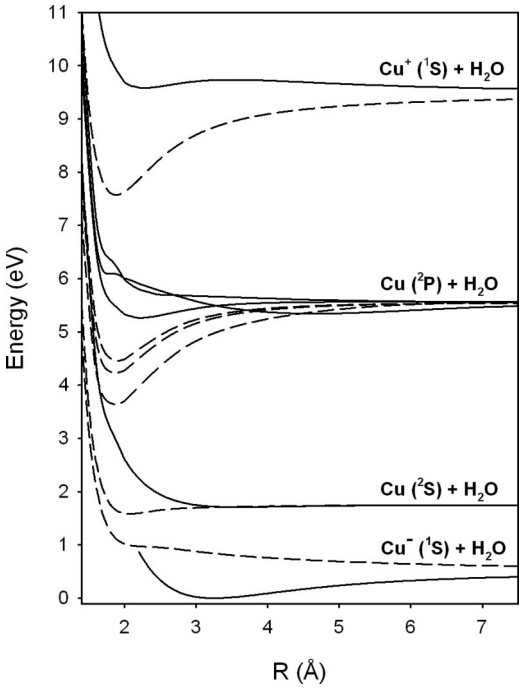

FIG. 2. Radial slices through the anion, neutral, excited state, and cation $Cu(H_2O)$ potential energy surfaces as a function of the distance between Cu and O. $Cu(H_2O)$ is constrained to either the C_{2v} Cu-H_2O (solid line) or the C_{2v} Cu-OH_2 (dotted lines) configuration. The anion, neutral, and cation curves are calculated at MP2/(aug-SDB aug-cc-pVTZ) and the excited state curve is calculated as the vertical excitation from the neutral $Cu(H_2O)$ geometries using time-dependent density functional theory. The neutral, excited state and cation curves are each shifted by a constant value ($+0.34$ eV, -0.33 eV, and -0.06 eV) in order for the asymptotic limits of the curves to match the experimentally determined atomic Cu electron affinity, $4\,^2P \leftarrow 4\,^2S$ transition energy and ionization potential.

Radial slices through the anion, neutral, excited state, and cation $Cu(H_2O)$ potential energy surfaces for the Cu-H_2O and Cu-OH_2 C_{2v} configurations are displayed in Fig. 2. The electronic transition of $Cu(H_2O)$ that is probed in the experiments described in Paper I correlates to the $4\,^2P \leftarrow 4\,^2S$ transitions of atomic copper, which fall at 3.79 and 3.82 eV (or 327.4 and 324.8 nm), respectively. Experimental[29–33] and computational[28] studies of excited states of metal-polar solvent complexes have shown that transitions such as Cu ($4\,^2P \leftarrow 4\,^2S$) are redshifted from that of the free atom, due to interaction with the solvent molecule. Our TDB3LYP calculations show that, as expected, the three P-states, degenerate in the free copper atom, are split into three nondegenerate electronic states with energies that depend on the orientation of the *p* orbital on Cu relative to the H_2O molecule. We note that the configurations near the Cu-OH_2 minimum, at small copper water separations, have the transition redshifted by as much as 1.91 eV compared to isolated copper atom. In the photodetachment-photoionization experiments described in Paper I, this shifting of the transition energy means that a probe (excitation) photon can only excite a neutral complex that samples a restricted range of H_2O orientation.

The radial slices of the $Cu^+(H_2O)$ potential energy sur-

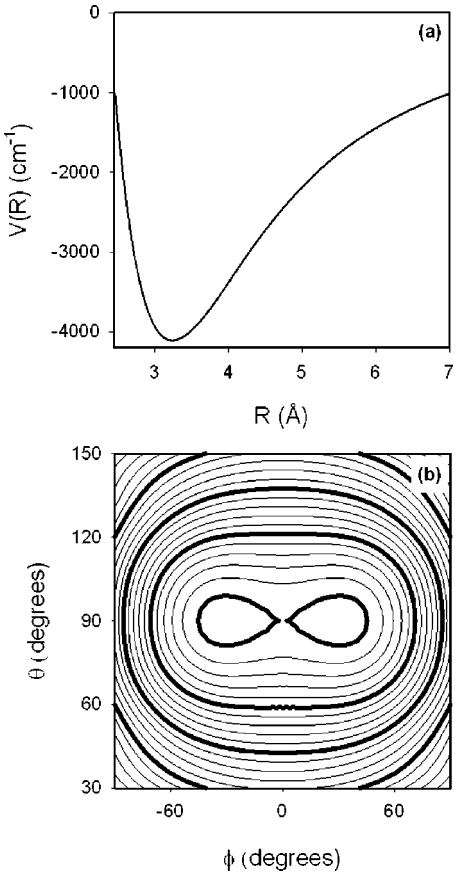

FIG. 3. Slices through the $Cu^-(H_2O)$ potential energy surface (a) as a function of the distance between Cu and the center of mass of water, R, with $\theta=90°$ and $\phi=0°$ and (b) as a function of θ and ϕ, minimizing with respect to R. In this contour plot, the thin contours are spaced by 200 cm^{-1} and the lowest energy contour is at -4000 cm^{-1}. In both cases, the zero in energy corresponds to $Cu^- + H_2O$ and the complex is bound by 4300 cm^{-1}.

face in Fig. 2 show that the Cu-OH_2 configurations are stabilized and the Cu-H_2O configurations are destabilized with respect to free Cu^+ and H_2O. We observe that the radial $Cu^+(H_2O)$ slice corresponding to Cu-H_2O does not decrease monotonically with increasing copper water distances, as may be initially expected. Instead, there is a local maximum at 3.5 Å and a local minimum at 2.3 Å. Harmonic frequency analysis shows a first-order saddle point at 2.28 Å, with the imaginary mode being the out-of-plane H_2O rotation. This feature can be understood using simple electrostatic principles. As H_2O approaches Cu^+ there is a competition between the repulsion of the ion and the positive end of the water dipole and the attraction between the ion and the water quadrupole moment (the oxygen has a slight negative charge). Near 2.3 Å, the attractive interaction causes a slight dip in the repulsive curve, without being able to create a true minimum.

C. Characterization of $Cu^-(H_2O)$

The radial and angular slices through the $Cu^-(H_2O)$ potential are plotted in Fig. 3. The equilibrium geometry of the complex corresponds to a hydrogen-bonded structure with a Cu^--H-O angle of 156.7°. The barrier between the two equivalent hydrogen-bonded structures is 166 cm^{-1}. As can be seen in the cuts through the potential, the anion potential is very flat in the region near the hydrogen-bonded configurations. For angular ranges outside those plotted in Fig. 3, the potential surface continues to rise monotonically.

Based on a comparison between the height of the barrier between the hydrogen-bonded minimum energy configurations and the harmonic frequency of the in-plane bend mode of 245 cm^{-1}, reported in Table III, we expect that there will be at least two states with energies below this barrier and they will manifest themselves as a tunneling doublet. This is confirmed by comparing the 51 cm^{-1} difference between the states with zero and one quanta of excitation in this mode with the 177 cm^{-1} difference between states with one and two quanta and the 176 cm^{-1} difference between the states with two and three quanta.[48] The fundamental frequencies for the in-plane bend of $Cu^-(H_2O)$ and $Cu^-(D_2O)$, reported in Table III, are obtained by subtracting the average of the energies of the states with zero and one quanta from the energy of the state with two quanta. The anharmonic nature of the anion potential energy surface in the in-plane bend coordinate necessitates variational calculation of the vibrational energies rather than by harmonic analysis. For the states with two quanta in the in-plane bend, the most probable configuration for both $Cu^-(H_2O)$ and $Cu^-(D_2O)$ corresponds to the C_{2v} transition state geometry. This further reflects that these states are above the isomerization barrier. Similar trends are observed for the stretch/bend combination bands.

In our simulations of the photoelectron-photoionization signals of $Cu^-(H_2O)$, we initiate the dynamics from the ten lowest energy states of the anion. These states have between zero and three quanta in both of the copper-water stretch and in the in-plane bend. In all cases, the states have zero quanta in the out-of-plane bend. The probability amplitudes for the stretch and bend overtone states show that these states sample configurations that correspond to $2.75\,\text{Å} < R < 3.75\,\text{Å}$; $-60° < \phi < 60°$ and $50° < \theta < 130°$. As the angular and radial dependences of these wave functions are nearly separable, the full eigenstates are very well represented by direct products of the one-dimensional stretch and bend functions.

D. Characterization of Cu(H_2O)

As mentioned above, the calculated surface for the neutral is obtained by first calculating the 16 slices through the Cu(H_2O) potential at fixed copper-water orientations and fitting these slices to Eq. (9). In these fits we only include points on the inner wall of the potential with $V(R,\theta,\phi) < -3V_{\min}$. This provides us with roughly two to three times as many potential points as parameters in the fit. In spite of this we find that the parameters are correlated. As such, the parameters are allowed to vary until we obtain a physically reasonable set of parameters for each cut. For example, we require R_M and R_S to be located near the minimum in the potential and the point of inflection on the outer wall of the potential. In all cases, the differences between the fit and calculated points for the radial cuts are smaller than 2 cm^{-1}, while the global surface reproduces the fit slices, by design.

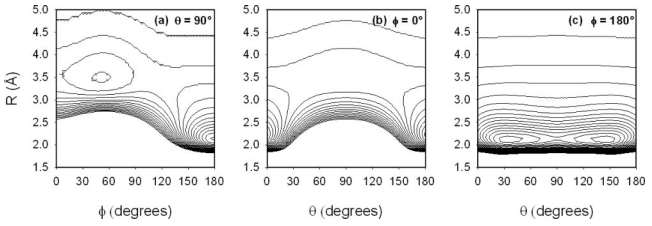

FIG. 4. Slices through the $Cu(H_2O)$ potential (a) as a function of R and ϕ with $\theta=90°$, (b) and (c) as a function of R and θ with $\phi=0°$ and 180°. The thin contours are spaced by 100 cm^{-1}. In all cases, the zero in energy corresponds to $Cu+H_2O$.

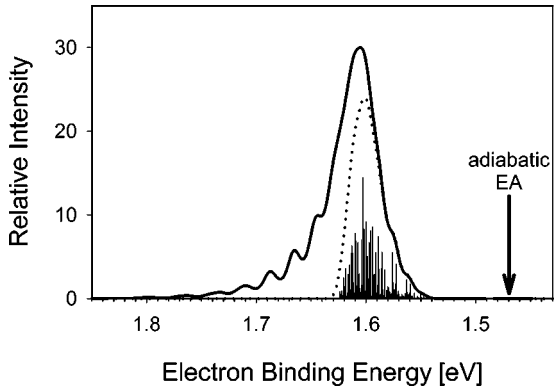

FIG. 5. Electron binding energy of $Cu^-(H_2O)$ at a vibrational temperature of 200 K. The solid line represents the full photoelectron spectrum. The dotted line represents the part of the spectrum that results from bound to bound transitions and is obtained by convoluting the stick spectrum with a Gaussian with FWHM= 80 cm^{-1}, as described in the text. The vertical arrow shows the location of the calculated (1.47 eV) adiabatic electron affinity of $Cu(H_2O)$, 0.14 eV below the vertical detachment energy, the peak of photoelectron spectrum. There will be no detectable photoelectron signal at energies corresponding to the adiabatic electron affinity.

The calculated points and the values for the parameters in the fit of the potential are available electronically.[48] Once these slices are fit, the potential is evaluated by first evaluating each of the 16 angular slices at the desired value of R. The angular dependence is obtained by taking the value of the potential for the 16 copper-water orientations and performing an inversion to a 16 term expansion of the potential of the form given in Eq. (5). In this case, $m \leqslant l \leqslant m+4$ in increments of 2 when $m \neq 0$, and when $m=0$,l can be 0, 2, 4, or 6.

Two-dimensional slices through the fit neutral surface are presented in Fig. 4. We perform variational calculations of all of the bound state energies and wave functions for $Cu(H_2O)$ and $Cu(D_2O)$. For the H_2O complex, the ground state is bound by 1113 cm^{-1} and the potential supports more than 311 bound states. For the D_2O complex, the ground state is bound by 1193 cm^{-1} while there are 160 states that are bound by at least 3 cm^{-1}. At low energies, all of the states are localized in the Cu-OH_2 minimum in the potential.

The calculated energies and assignments of states that have energies that are below one half of the dissociation energy of the ground state are reported for $Cu(H_2O)$ and $Cu(D_2O)$ in EPAPS.[48] All of these states display clean nodal patterns and are easily assigned in terms of the number of quanta in the copper-water stretch, in-plane and out-of-plane bends. As was the case for the anion, at low levels of bend excitation, the system displays distinct double-well character. In contrast to the anion, the double-well behavior is manifested in the out-of-plane bend and three and four states are trapped below the barrier between the two equivalent minima for the H_2O and D_2O complexes, respectively. Finally, in contrast to the anion, there is strong coupling between the three vibrational modes. This is also manifested in the dependence of the effective out-of-plane bend frequencies on the level of stretch excitation.[48]

The above discussion has focused on states that are localized in the Cu-OH_2 potential minimum. In the photodetachment-photoionization experiments, the states that are probed are those that have nonzero overlap with the populated vibrational states of the anion. In spite of the fact that these states sample fairly large regions of configuration space, their overlaps with the states described above are nearly zero. To investigate the states that contribute to the signal, we evaluate the photoelectron spectrum from the time-dependent wave packets described in Paper I. For these calculations, we first evaluate the autocorrelation function

$$C_n(t)=\langle \Psi_n | e^{-i(\hat{H}_N-\hat{H}_A)t/\hbar} | \Psi_n \rangle \tag{11}$$

for each of the ten initial states, represented by Ψ_n, used in the simulation. Here, $\hat{H}_A$ and $\hat{H}_N$ represent Hamiltonians for the anion and neutral charge states of the copper-water complex. The spectrum is related to $C_n(t)$ by a Fourier transform.[61] We then take the weighted average of the spectra for each of the initial states, weighting the results by the Boltzmann factor. In all cases, the energy scale is the electron binding energy, expressed in electron volts. The spectrum is calculated for a vibrational temperature of $Cu^-(H_2O)$ of 200 K and is plotted in Fig. 5. To facilitate comparison with experiment, the calculated spectrum has been convoluted with a Gaussian that has a full width at half maximum (FWHM) of 80 cm^{-1}. We also calculated the corresponding stick spectrum at this temperature by taking the square of the overlap of the wave functions of the anion with the bound wave functions of the neutral, weighted by the appropriate Boltzmann factor. Comparing the spectrum obtained by convoluting the stick spectrum with a Gaussian with a FWHM of 80 cm^{-1} and the spectrum obtained from the correlation function, we find that 50% of the intensity arises from bound to bound transitions. We note that although there is a rapid onset of the signal at roughly 1.58 eV, this energy is more than 0.1 eV above the adiabatic electron affinity of $Cu(H_2O)$, calculated to be 1.47 eV by taking the energy difference between the lowest energy vibronic states of $Cu(H_2O)$ and $Cu^-(H_2O)$. Finally, the calculated photoelectron spectrum exhibits peaks well above the dissociative photodetachment onset. Such peaks could not have been resolved in the earlier experiments of Misaizu and co-workers,[23,24] but they may have been observed in very recent photoelectron imaging experiments in our laboratory.

E. Characterization of $Cu^+(H_2O)$

We calculate two potential energy surfaces that describe $Cu^+(H_2O)$: a relaxed $Cu^+(H_2O)$ surface in the region of the

$Cu^+(H_2O)$ minimum in which the energy is minimized with respect to the three intramolecular coordinates of water, and a global vertical ionization surface using the geometries of the neutral Cu(H_2O) complexes. The former is used to calculate the vibrational wave functions for $Cu^+(H_2O)$ and the latter is used to interpret the photodetachment-photoionization experiments in Paper I. For brevity we do not display the relaxed surface, but use it to illustrate the necessity of such full surface calculations in accurately predicting the vibrational frequencies for such complexes. The results of a harmonic analysis, presented in Table III, predict an out-of-plane bending frequency (excitation in θ) to be 30 cm^{-1}, but variational calculations using the complete relaxed surface predict a frequency of 197 cm^{-1}. Inspection of the relaxed surface along θ shows that the potential is essentially flat for $\theta \leqslant 60°$, only rising 60 cm^{-1} from the minimum over this range of angles. As a result, harmonic frequency analysis predicts an out-of-plane bending frequency that is much smaller than the energy of the fundamental in this mode. This illustrates that variational calculations are essential to accurately calculate the vibrational frequencies of molecules having anharmonic potential energy surfaces.

In the experiments described in Paper I,[1] the dynamics of neutral Cu(H_2O) is monitored in real time by femtosecond multiphoton ionization of the time-evolving neutral complexes. As discussed, correct interpretation of these time-dependent $Cu^+(H_2O)$ signals requires simultaneous consideration of both the excitation and ionization processes involved in the probe step of the experiments. We have discussed the variation of the excitation energy as a function of Cu(H_2O) geometry, and now we turn to the vertical ionization energy of Cu(H_2O). Two cuts through the vertical ionization surface are presented in Fig. 6. For ease of interpretation, we display ionization energy contours above and below the copper atom ionization potential (7.73 eV) as dotted and solid lines, respectively. Figure 6(a) clearly shows that as the positive or negative end of the water dipole points toward copper the ionization energy, respectively, increases or decreases with respect to the copper atom. This marked variation in the ionization energy of the complex as its geometry varies has profound consequences for the photodetachment-photoionization experiments that we report in Paper I.[1] It provides selectivity in the ranges of Cu(H_2O) geometries that are ionized in these experiments, and as a consequence, the time-dependent photodetachment-photoionization signals can be used to develop pictures of the dynamics of neutral Cu(H_2O) as a function of time.

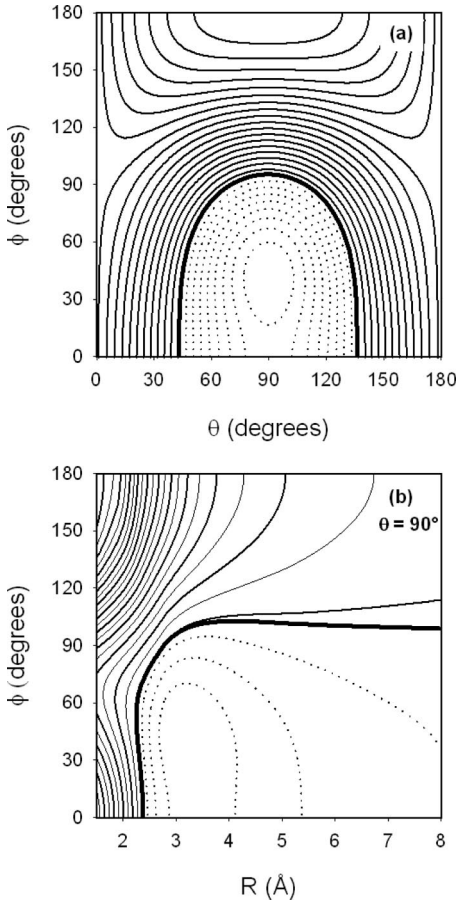

FIG. 6. Slices through the vertical ionization surface for Cu(H_2O) calculated at MP2/(aug-SDB aug-cc-pVTZ), and shifted by -0.06 eV to reproduce the ionization potential of Cu asymptotically. In (a) the surface is plotted as a function of θ and ϕ for $R=3.0$ Å increments of 0.04 eV, where the highest contour represents 8.04 eV, while in (b) it is plotted as a function of R and ϕ for $\theta=90°$, in increments of 0.1 eV, where the highest contour represents 8.00 eV. In both cases, the thick solid line provides the ionization potential of Cu (7.73 eV), while dotted and thin solid lines represent larger and smaller ionization energies, respectively.

IV. CONCLUSIONS

In this paper, we have presented a computational and theoretical investigation into the potential energy surfaces and vibrational energies and wave functions of the anion, neutral, and cation Cu(H_2O) complexes. We find that $Cu^-(H_2O)$ is delocalized between two equivalent Cu-HOH hydrogen bonded minima, and that it has a dissociation energy of 0.39 eV. Vertical electron detachment from $Cu^-(H_2O)$ produces neutral Cu(H_2O) with an internal energy comparable to the Cu-H_2O dissociation energy, and as a result, some of the neutral complexes formed by this method will dissociate into Cu and H_2O. Our calculations show that electron photodetachment from $Cu^-(H_2O)$ produces neutral Cu(H_2O) initially far from its equilibrium geometry and consequently with excitation of H_2O internal rotation. The nascent neutral complexes thus undergo large-amplitude water reorientation and Cu-H_2O dissociation. We find that neutral Cu(H_2O) has a nonplanar equilibrium geometry and a dissociation energy of 0.16 eV. $Cu^+(H_2O)$ is found to have a planar C_{2v} geometry, and a dissociation energy of 1.74 eV.

We find that for each of the three charge states of Cu(H_2O), calculation of the potential energy surface followed by variational calculations are required to accurately characterize their vibrational wave functions and energies, due to anharmonicity in their potential energy surfaces. The photoelectron spectrum of $Cu^-(H_2O)$ is calculated for a 200 K vibrational temperature of the anion. Based on an analysis of this spectrum, 50% of the population is in vibronic states that have energies above the dissociation energy of the neutral complex. This estimate is borne out by the extensive

dissociation of neutral $Cu(H_2O)$ observed in the experiments in Paper I.

We use time-dependent density functional theory to investigate the variation of an electronic transition of the neutral $Cu(H_2O)$ complex which correlates to the $4\,^2P \leftarrow 4\,^2S$ transition of the copper atom. We find that this transition is blueshifted by up to 0.14 eV in Cu-HOH configurations and redshifted by up to 1.91 eV in $Cu\text{-}OH_2$ configurations, at small copper-water separations. Finally, the vertical ionization energies for $Cu(H_2O)$ are calculated as a function of the intermolecular coordinates. We find that, with respect to the IP of copper atom, the vertical ionization energy of neutral $Cu(H_2O)$ is blueshifted by up to 0.36 eV in Cu-HOH configurations and redshifted by as much as 1.87 eV in $Cu\text{-}OH_2$ configurations.

Additional experimental studies will complement the calculations we present in this paper on the anion, neutral, and cation $Cu(H_2O)$ complexes. First, the $Cu(H_2O)$ anion would be an excellent candidate for investigation by vibrational predissociation spectroscopy[3,6,62,63] which will further characterize its vibrational frequencies and potential energy surface. Second, a vibrationally resolved photoelectron spectrum of $Cu^-(H_2O)$ will characterize the nascent neutral $Cu(H_2O)$ formed by electron detachment of the anion. Resonant multiphoton ionization spectroscopy can be applied to characterize the vibrational frequencies, dissociation energies, and excitation energies of the excited states of the neutral $Cu(H_2O)$ complex.[29,31–33,64] Zero kinetic energy pulsed field ionization (ZEKE-PFI) photoelectron spectroscopy can be used to measure the ionization potential of neutral $Cu(H_2O)$, and the vibrational frequencies of $Cu^+(H_2O)$.[65–68]

In conclusion, our calculations on the three charge states of $Cu(H_2O)$ illustrate that $Cu(H_2O)$ is a rich system for experimental investigations. It is an excellent choice for investigation by femtosecond photodetachment-photoionization experiments. These experiments exploit the fact that the anion has a localized Cu-HOH configuration. In addition, there is a large difference in the shapes of the anion and neutral potential surfaces which gives rise to dynamics on the neutral surface following electron photodetachment from the anion. Finally, the vertical excitation and ionization energy of neutral $Cu(H_2O)$ vary significantly with the complex geometry, which allows time-resolved resonant multiphoton ionization to probe neutral $Cu(H_2O)$ in selected configurations.

ACKNOWLEDGMENTS

We gratefully acknowledge support from the National Science Foundation under Grants Nos. CHE0201848 and PHY0096822 (W.C.L.) and CHE-0200968 (A.B.M.), and the Air Force Office of Scientific Research Grant No. F49620-02-1-0371 (W.C.L.). This work was partially supported by National Computational Science Alliance under Grant No. CHE030010N and utilized the Origin2000 Array. A.B.M. was supported by the JILA Visiting Fellowship program. A.B.M. also acknowledges the Dreyfus Foundation awards program for partial support of this work.

[1] F. Muntean, M. S. Taylor, A. B. McCoy, and W. C. Lineberger, J. Chem. Phys. **121**, 5676 (2004), preceding paper.
[2] M. A. Duncan, Annu. Rev. Phys. Chem. **48**, 69 (1997).
[3] D. A. Wild and E. J. Bieske, Int. Rev. Phys. Chem. **22**, 129 (2003).
[4] M. A. Duncan, Int. Rev. Phys. Chem. **22**, 407 (2003).
[5] A. M. Ellis, Int. Rev. Phys. Chem. **20**, 551 (2001).
[6] W. H. Robertson and M. A. Johnson, Annu. Rev. Phys. Chem. **54**, 173 (2003).
[7] W. Kaim and J. Rall, Angew. Chem., Int. Ed. Engl. **35**, 43 (1996).
[8] E. I. Solomon, M. D. Lowery, D. E. Root, and B. L. Hemming, Adv. Chem. Ser. **246**, 121 (1995).
[9] E. I. Solomon, P. Chen, M. Metz, S.-K. Lee, and A. E. Palmer, Angew. Chem., Int. Ed. Engl. **40**, 4570 (2001).
[10] C.-G. Zhan and S. Iwata, Chem. Phys. Lett. **232**, 72 (1995).
[11] I. Pápai, J. Chem. Phys. **103**, 1860 (1995).
[12] J. Sauer, H. Haberlandt, and G. Pacchioni, J. Phys. Chem. **90**, 3051 (1986).
[13] M. W. Ribarsky, W. D. Luedtke, and U. Landman, Phys. Rev. B **32**, 1430 (1985).
[14] J. Miralles-Sabater, I. Garcia-Cuesta, M. Merchan, and I. Nebot-Gil, THEOCHEM **57**, 1 (1989).
[15] L. A. Curtiss and E. Bierwagen, Chem. Phys. Lett. **176**, 417 (1991).
[16] C. W. Bauschlicher, Jr., J. Chem. Phys. **84**, 260 (1986).
[17] M. R. A. Blomberg, U. B. Brandemark, and P. E. M. Siegbahn, Chem. Phys. Lett. **126**, 317 (1986).
[18] M. Rosi and C. W. Bauschlicher, Jr., J. Chem. Phys. **90**, 7264 (1989).
[19] M. Rosi and C. W. Bauschlicher, Jr., J. Chem. Phys. **92**, 1876 (1990).
[20] D. Feller, E. D. Glendening, and W. A. de Jong, J. Chem. Phys. **110**, 1475 (1999).
[21] C. W. Bauschlicher, Jr., S. R. Langhoff, and H. Partridge, J. Chem. Phys. **94**, 2068 (1991).
[22] L. A. Curtiss and R. Jurgens, J. Phys. Chem. **94**, 5509 (1990).
[23] F. Misaizu, K. Tsukamoto, M. Sanekata, and K. Fuke, Surf. Rev. Lett. **3**, 405 (1996).
[24] F. Misaizu, K. Tsukamato, M. Sanekata, and K. Fuke, Laser Chem. **15**, 195 (1995).
[25] J. W. Kauffman, R. H. Hauge, and J. L. Margrave, J. Phys. Chem. **89**, 3541 (1985).
[26] T. F. Magnera, D. E. David, D. Stulik, R. G. Orth, H. T. Jonkman, and J. Michl, J. Am. Chem. Soc. **111**, 5036 (1989).
[27] N. F. Dalleska, K. Honma, L. S. Sunderlin, and P. B. Armentrout, J. Am. Chem. Soc. **116**, 3519 (1994).
[28] P. Archirel, V. Dubois, and P. Maître, Chem. Phys. Lett. **323**, 7 (2000).
[29] J. Miyawaki, K.-I. Sugawara, H. Takeo, C. Dedonder-Lardeux, S. Martrenchard-Barra, C. Jouvet, and D. Solgadi, Chem. Phys. Lett. **302**, 354 (1999).
[30] R. Takasu, K. Nishikawa, N. Miura, A. Sabu, K. Hashimoto, C. P. Schulz, I. V. Hertel, and K. Fuke, J. Phys. Chem. A **105**, 6602 (2001).
[31] P. Brockhaus, I. V. Hertel, and C. P. Schulz, J. Chem. Phys. **110**, 393 (1999).
[32] C. Nitsch, C. Hüglin, I. V. Hertel, and C. P. Schulz, J. Chem. Phys. **101**, 6559 (1994).
[33] C. P. Schulz and C. Nitsch, J. Chem. Phys. **107**, 9794 (1997).
[34] M. J. Frisch. G. W. Trucks, H. B. Schlegel *et al.*, GAUSSIAN 98, Gaussian, Inc., Pittsburgh, PA, 1998.
[35] X.-B. Wang, L.-S. Wang, R. Brown, P. Schwerdtfeger, D. Schröder, and H. Schwarz, J. Chem. Phys. **114**, 7388 (2001).
[36] M. Dolg, U. Wedig, H. Stoll, and H. Preuss, J. Chem. Phys. **86**, 866 (1987).
[37] T. H. Dunning, Jr., J. Chem. Phys. **90**, 1007 (1989).
[38] R. E. Stratmann, G. E. Scuseria, and M. J. Frisch, J. Chem. Phys. **109**, 8218 (1998).
[39] M. E. Casida, C. Jamorski, K. C. Casida, and D. R. Salahub, J. Chem. Phys. **108**, 4439 (1998).
[40] J. Guan, M. E. Casida, and D. R. Salahub, J. Mol. Struct.: THEOCHEM **527**, 229 (2000).
[41] F. C. De Lucia, P. Helminger, R. L. Cook, and W. Gordy, Phys. Rev. A **5**, 487 (1972).
[42] R. N. Zare, *Angular Momentum: Understanding Spatial Aspects in Chemistry and Physics* (Wiley, New York, 1988).
[43] Z. Bačić and J. C. Light, Annu. Rev. Phys. Chem. **40**, 469 (1989).
[44] D. T. Colbert and W. H. Miller, J. Chem. Phys. **96**, 1982 (1992).
[45] W. H. Press, B. P. Flannery, S. A. Teukolsky, and W. T. Vetterling, *Numerical Recipes* (Cambridge University Press, New York, 1986).

[46] Z. Bačić, R. M. Whitnell, D. Brown, and J. C. Light, Comput. Phys. Commun. **51**, 35 (1988).
[47] H.-S. Lee and A. B. McCoy, J. Chem. Phys. **116**, 9677 (2002).
[48] See EPAPS Document No. E-JCPSA6-121-013434 for (1) the *ab initio* energies used to construct the anion, neutral and cation Cu(H_2O) potential energy surfaces, and (2) the twenty lowest bound vibronic states of the anion and neutral, Cu(H_2O) and Cu(D_2O). A direct link to this document may be found in the online article's HTML reference section. The document may also be reached via the EPAPS homepage (http://www.aip.org/pubservs/epaps.html) or from ftp.aip.org in the directory /epaps/. See the EPAPS homepage for more information.
[49] W. C. Martin, J. R. Fuhr, D. E. Kelleher *et al.*, *NIST Atomic Spectra Database*, 2.0 ed. (National Institute of Standards and Technology, Gaithersburg, MD, 2002).
[50] M. S. Taylor, Ph.D Thesis, University of Colorado, Boulder, 2004.
[51] S. F. Boys and F. Bernardi, Mol. Phys. **19**, 553 (1970).
[52] S. S. Xantheas, J. Chem. Phys. **104**, 8821 (1996).
[53] C. W. Bauschlicher, Jr., J. Chem. Phys. **100**, 1215 (1994).
[54] C. W. J. Bauschlicher, S. R. Langhoff, H. Partridge, and M. Sodupe, J. Phys. Chem. **97**, 856 (1993).
[55] J. Hrušák, W. Koch, and H. Schwarz, J. Chem. Phys. **101**, 3898 (1994).
[56] T. H. Dunning, Jr., J. Phys. Chem. A **104**, 9062 (2000).
[57] K. Pierloot, B. Dumez, P.-O. Widmark, and B. O. Roos, Theor. Chim. Acta **90**, 87 (1995).
[58] C. W. Bauschlicher, S. R. Langhoff, H. Partridge, and L. A. Barnes, J. Chem. Phys. **91**, 2399 (1989).
[59] J. M. L. Martin and A. Sundermann, J. Chem. Phys. **114**, 3408 (2001).
[60] Fuke and co-workers (Refs. 23 and 24) derive a value of $D_0[Cu^-(H_2O)]=0.55$ eV using the thermochemical cycle: $D_0[Cu^-(H_2O)]=DE[Cu(H_2O)]+VDE[Cu^-(H_2O)]-EA[Cu]$, where EA [Cu] is the electron affinity of atomic copper, VDE[Cu-(H_2O)] is the measured vertical detachment energy of $Cu^-(H_2O)$ and DE[Cu(H_2O)] is the energy required to separate neutral Cu(H_2O) starting from the anion geometry. For DE[Cu(H_2O)], they used a value of 0.2 eV, the calculated binding energy of equilibrium Cu(H_2O) in its minimum energy configuration. Using the more appropriate value of DE[Cu(H_2O)]=0.05 eV, the binding energy of neutral Cu(H_2O) at the anion geometry, we obtain $D_0[Cu^-(H_2O)]=0.39$ eV.
[61] E. J. Heller, Acc. Chem. Res. **14**, 368 (1981).
[62] J.-H. Choi, K. T. Kuwata, Y.-B. Cao, and M. Okumura, J. Phys. Chem. A **102**, 503 (1998).
[63] M. S. Johnson, K. T. Kuwata, C.-K. Wong, and M. Okumura, Chem. Phys. Lett. **260**, 551 (1996).
[64] J. Miyawaki and K.-I. Sugawara, J. Chem. Phys. **118**, 2173 (2003).
[65] J. Miyawaki and K.-I. Sugawara, J. Chem. Phys. **119**, 6539 (2003).
[66] J. Miyawaki, D.-S. Yang, and K.-I. Sugawara, Chem. Phys. Lett. **372**, 627 (2003).
[67] K. Wang, D. A. Rodham, V. McKoy, and G. A. Blake, J. Chem. Phys. **108**, 4817 (1998).
[68] D. A. Rodham and G. A. Blake, Chem. Phys. Lett. **264**, 522 (1997).
[69] R. C. Bilodeau, M. Scheer, and H. K. Haugen, J. Phys. B **31**, 3885 (1998).
[70] D. R. Lide, in *Handbook of Chemistry and Physics*, edited by D. R. Lide (CRC, New York, 1995), p. 10.